Northumbria Research Link

The Contralateral Delay Activity Tracks the Sequential Loading of Objects into Visual Working Memory, Unlike Lateralized Alpha Oscillations

Sisi Wang[1,2*], Jason Rajsic[1*], and Geoffrey F. Woodman[1]

Abstract

■ Visual working memory temporarily represents a continuous stream of task-relevant objects as we move through our environment performing tasks. Previous work has identified candidate neural mechanisms of visual working memory storage; however, we do not know which of these mechanisms enable the storage of objects as we sequentially encounter them in our environment. Here, we measured the contralateral delay activity (CDA) and lateralized alpha oscillations as human subjects were shown a series of objects that they needed to remember. The amplitude of CDA increased following the presentation of each to-be-remembered object, reaching asymptote at about three to four objects. In contrast, the concurrently measured lateralized alpha power remained constant with each additional object. Our results suggest that the CDA indexes the storage of objects in visual working memory, whereas lateralized alpha suppression indexes the focusing of attention on the to-be-remembered objects. ■

INTRODUCTION

Visual working memory continuously represents new information for ongoing cognitive tasks as we move through our environment (Cowan, 2001; Baddeley & Hitch, 1974). Previous work suggests that both the contralateral delay activity (CDA) and alpha suppression may index visual working memory storage (Adam, Robison, & Vogel, 2018; Luria, Balaban, Awh, & Vogel, 2016; Sander, Werkle-Bergner, & Lindenberger, 2012; Sauseng et al., 2009; McCollough, Machizawa, & Vogel, 2007; Vogel & Machizawa, 2004). However, given the intertwined nature of working memory storage and other cognitive processes (e.g., attentional selection, Cowan, 2001), it is possible that the CDA and alpha power suppression index separate cognitive mechanisms. Indeed, a recent study suggests that these neural indices may be dissociable by manipulating task demands (Hakim, Adam, Gunseli, Awh, & Vogel, 2019). In this study, we test the novel prediction that if these are both electrophysiological markers of visual working memory storage, then we should see them both systematically increase as we sequentially load information into visual working memory.

The CDA is a sustained negative potential at posterior electrodes contralateral to remembered visual objects (Vogel, McCollough, & Machizawa, 2005; Vogel & Machizawa, 2004). The other neural metric of visual working memory storage that has been proposed is lateralized alpha power suppression measured across posterior electrodes contralateral to to-be-remembered stimuli (Sauseng et al., 2009; but see Fukuda, Kang, & Woodman, 2016). Although some have proposed that this lateralized alpha suppression indexes the allocation of covert attention (e.g., Kelly, Lalor, Reilly, & Foxe, 2006; Thut, Nietzel, Brandt, & Pascual-Leone, 2006; Sauseng et al., 2005; Worden, Foxe, Wang, & Simpson, 2000), others have found changes in lateralized alpha power as memory set size increases (Adam et al., 2018; Sander et al., 2012; Sauseng et al., 2009), suggesting that lateralized alpha also measures visual working memory storage (Sauseng et al., 2009; but see Fukuda et al., 2016).

Our goal in this study was to use sequentially presented memory sets to understand the cognitive mechanisms underlying the CDA and lateralized alpha suppression. The sequential presentation of memory items has been frequently used in studies of verbalizable materials to understand how information is loaded into working memory (Broadbent & Broadbent, 1981; Baddeley & Hitch, 1974; Sternberg, 1969; Conrad, 1964; Brown, 1958). Moreover, to support ongoing cognitive operations in daily life, visual working memory needs to be able to handle information that is acquired from the environment through time as new objects are fixated or disappear from view. Therefore, the present methods allow us to make the following predictions about how any neural metric of working memory should behave. If one or both of these neural indices reflect visual working memory storage and maintenance, then we should see

[1]Vanderbilt University, [2]East China Normal University, Shanghai, China

*These authors contributed equally to this work.

Journal of Cognitive Neuroscience 31:11, pp. 1689–1698
https://doi.org/10.1162/jocn_a_01446

the amplitude of the effect step with each successive item in a sequential memory set, until visual working memory filled and capacity is reached. However, if one or both of these metrics instead reflect the focusing of attention on items as they are encoded, then it should remain constant as each successive item is presented, because only one item needs to be attended at a time in the memory task we used here (see Figure 1). To determine the generality of our findings and replicate the pattern of results with another type of stimulus, we presented to-be-remembered colored rectangles or letters on different trials.

METHODS

Participants

Participants were recruited from Vanderbilt University and the surrounding community. All participants gave informed consent and completed the task for $15/hr in compensation. All self-reported normal or corrected-to-normal visual acuity and normal color vision. Data were collected from 30 participants, but 10 participants were excluded due to excessive eye movement and muscular artifacts (more than 25% trials rejected due to artifacts), and one more participant was excluded due to chance-level performance (48% correct across set sizes), leaving 19 participants (13 women, M_{age} = 22.8 years, SD_{age} = 5.7 years) in the final data set. The relatively high rate of trial rejection was due to participants needing to maintain strict fixation during the long trials (i.e., up to 6–7 sec) and our stringent criteria for inclusion (described below).

Stimuli and Procedures

Stimuli were presented using MATLAB (R2017b 9.3.0; MathWorks) and the Psychophysics Toolbox (Version 3.0.12; Brainard, 1997; Pelli, 1997) on a 24-in. LED monitor (ASUS VG 248; 120 Hz refresh rate). Participants were seated approximately 100 cm from the screen. Stimuli were presented on a gray background (x = 275, y = 448, L = 35 cd/m^2, x and y define chromaticity, L represents luminance in the CIE xyY color space derived from the CIE 1931 color space).

Each trial began with a display containing a white fixation cross (x = 336, y = 346, L = 235 cd/m^2, 0.2° of visual angle) in the center of the screen (for 500 msec), followed by a white arrow cue (0.8° of visual angle wide and 0.4° tall), indicating the relevant side of the screen (right or left) to be attended (100 msec). Participants were instructed to attend to the upcoming items appearing in the same hemifield as the cue direction, keeping their eyes fixed on the center fixation. After a postcue delay (900 msec), participants were shown bilateral pairs of one, three, or six sequentially presented colored rectangles or letters, such that they needed to encode a single item in the attended hemifield with each stimulus onset. Each bilateral pair of items appeared on the screen for 100 msec, and the interval between each successive

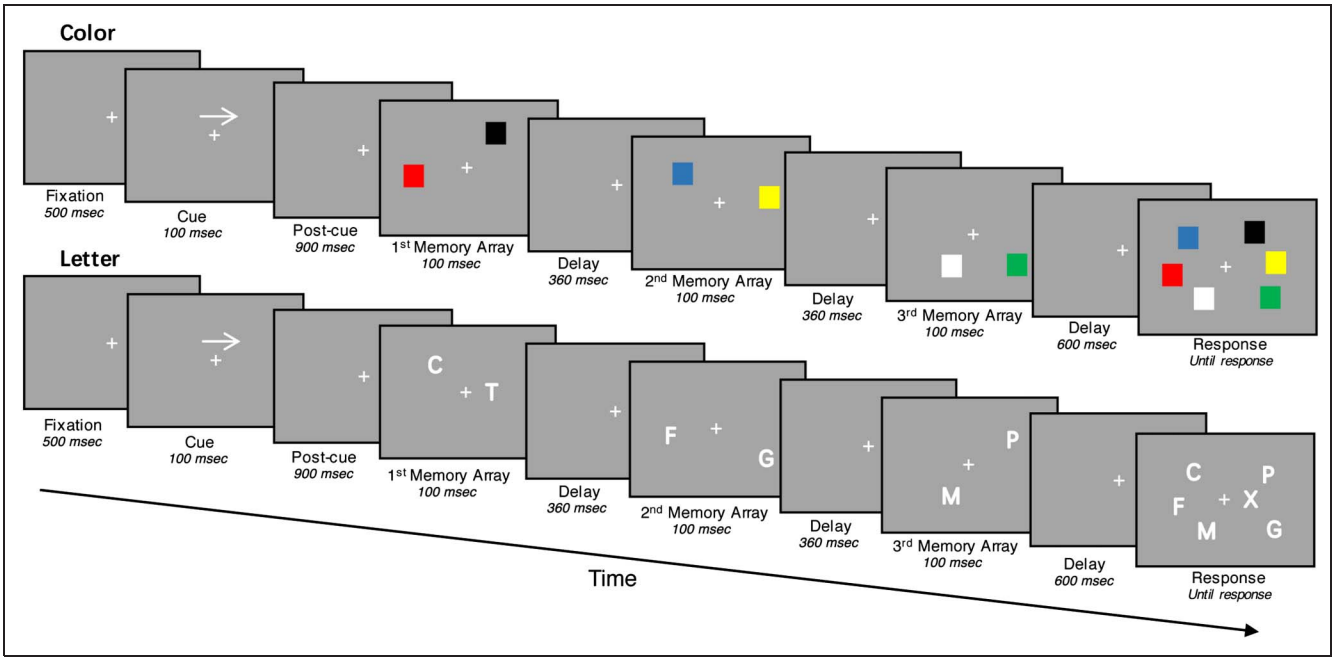

Figure 1. Illustration of the experimental paradigm. An example of the sequential working memory task from an individual trial with set size 3 in which the memoranda were colored rectangles (top) and letters (bottom). The cue arrows in the example trials point to the right side, instructing participants to attend to the upcoming items appearing in the right hemifield, keeping their eyes fixed on the center fixation. Participants then pressed one button on a handheld game pad to indicate whether one of the objects had changed or not in the right hemifield of the test array. The colors of the test array stayed the same in the color example trial, whereas one of the letters in the test array changed in the letter example trial. The memory trials could contain one, three, or six memory items.

display was 360 msec, with a 600-msec delay period following the last pair of items. For a given trial, all items were either colored rectangles or letters. The test array consisted of all the items sequentially presented in one trial and one item in both the task-relevant or task-irrelevant hemifield could change with a probability of 50%. On a change trial, one of the colored rectangles would change to a color not previously seen in that hemifield on that trial or one of the letters would change to another letter not previously seen in that hemifield on that trial. The locations of all the items in the test array stayed the same as they appeared in the memory arrays, including the changed item. Participants were instructed only to report changes in the task-relevant hemifield. Participants then pressed one button on a handheld game pad to indicate that one of the objects had changed and a different button to indicate that all items had stayed the same. The meaning of these buttons was randomized across participants.

Colors of the rectangles were chosen from a pool of eight distinct colors: red ($x = 625$, $y = 352$, $L = 40$ cd/m^2), green ($x = 275$, $y = 656$, $L = 116$ cd/m^2), blue ($x = 142$, $y = 72$, $L = 9$ cd/m^2), magenta ($x = 356$, $y = 194$, $L = 42$ cd/m^2), yellow ($x = 448$, $y = 507$, $L = 218$ cd/m^2), gray ($x = 215$, $y = 298$, $L = 18$ cd/m^2), white ($x = 336$, $y = 346$, $L = 235$ cd/m^2), and black ($x = 319$, $y = 315$, $L = 0.6$ cd/m^2). Letters were chosen from a pool of eight distinct uppercase consonants appearing in Arial font (C, F, M, P, S, T, V, or X), colored in white (255 255 255, $L = 330$ cd/m^2). Sets of colors and letters were randomly chosen from the color pool or the letter pool, without replacement for the items in a given hemifield. Sizes of the two types of stimuli were equated to approximate a mean of 0.34° of visual angle wide and 0.4° tall. They were placed along the circumference of one of three progressively eccentric imaginary circles (2°, 3.8°, 5.5° radius), centered on fixation and randomly placed in the left or right hemifield. Of course, any two objects presented in a trial could not share the same location. All the stimulus types (colored rectangles and letters) and set size (1, 3, and 6) were randomly interleaved within a given block, ensuring that both set size and stimuli type varied randomly from trial to trial. All the participants completed 192 trials with each type of to-be-remembered stimulus and set size for 1152 trials in total.

EEG Acquisition

The electroencelphalogram was recorded in an electrically shielded, soundproof booth from 30 active Ag/AgCl electrodes (Brain Products actiCHamp) mounted in an elastic cap positioned according to the International 10–20 system (Fp1, Fp2, Fz, F3, F4, F7, F8, FC5, FC6, C3, C4, Cz, T7, T8, P7, P8, P3, P4, Pz, PO7, PO8, PO3, PO4, POz, O1, O2, Oz). Two additional electrodes were affixed with stickers to the left and right mastoids, and a ground electrode was placed in the elastic cap at Fpz. Eye movements and blinks were monitored using EOG activity. We collected EOG data with two horizontal EOG (HEOG) electrodes placed ~1 cm from the left and right outer canthi and one vertical EOG electrodes placed below the right eye. Data were referenced online to the right mastoid and re-referenced offline to the algebraic average of the left and right mastoids. Incoming data were filtered from 0.01 to 100 Hz and recorded with a 250 Hz sampling rate. Impedance values were kept below 5 kΩ.

EEG Analysis

Artifact Rejection

Trials including artifacts due to blinks, amplifier saturation, or excessive noise were first rejected using a standard trial-rejection function from the EEGLAB Toolbox (*eegthresh.m*; Delorme & Makeig, 2004). If the maximum voltage during the 1-sec interval surrounding each to-be-remembered stimulus was greater than +100 μV or the minimum voltage was less than −100 μV, it was marked as an artifact and rejected. Next, we performed a two-step procedure to reject trials based on the presence of systematic horizontal eye movements below this threshold, because these eye movements could contaminate our lateralized measures. First, we used a split-half sliding window approach (Adam et al., 2018; window size = 200 msec, step size = 20 msec, threshold = 20 μV) on the HEOG signal. We slid a 200-msec time window in steps of 20 msec from the beginning to the end of the trial. If the change in voltage from the first half to the second half of the window was greater than 20 μV, it was marked as an eye movement and rejected. Four participants with fewer than 75% trials remaining were excluded following this step. Because of the limited signal-to-noise ratio of EOG recordings, trials with consistent, small eye movements could not be reliably detected and rejected by the first step but were caught during the second step. In the second step, we calculated the averaged HEOG for left and right cue trials (Woodman & Luck, 2003). If this averaged HEOG exceeded ±5 μV, then the participant was excluded from the analyses. We adopted a slightly higher threshold than the 3 μV adopted by Woodman and Luck (2003) because the longer presentation durations for set sizes 3 and 6 were more prone to low-frequency noise pushing the waveforms near threshold. This led to the exclusion of six more participants. For the remaining participants, an average of 5.14% ($SD = 4.79$%) of trials were excluded.

Contralateral Delay Activity

To measure the CDA, we baseline-corrected the signal to the mean of the 200 msec before the onset of the first memory array. Lateralized waveforms were computed by subtracting the activity of the ipsilateral electrodes from the activity of the contralateral electrodes across

the lateral-occipital and posterior-parietal electrodes: P3, P4, P7, P8, PO3, PO4, PO7, PO8, O1, and O2. Statistics were performed on the baseline-corrected, but unfiltered data so that filtering would not distort the timing and amplitudes of the waveforms. For visualization purposes, trials were low-pass filtered with a two-way least squares finite impulse response filter function from the EEGLAB Toolbox (*eegfilt.m*; Delorme & Makeig, 2004) with a low-pass filter of 30 Hz.

Lateralized Alpha Power Analysis

To measure lateralized alpha power, we first bandpass-filtered the raw EEG data using the eegfilt.m function and then applied the MATLAB Hilbert transform (*hilbert.m*) to extract the instantaneous power values for the alpha band (8–12 Hz). Percent change in alpha power was calculated relative to a baseline period before the onset of the cue (−1400 to −1000 msec relative to the first memory array onset; Adam et al., 2018). Finally, lateralized alpha power was calculated by subtracting the change in alpha power for ipsilateral electrodes from the change of alpha power for contralateral electrodes across the same lateral-occipital and posterior-parietal electrodes we used to measure the CDA: P3, P4, P7, P8, PO3, PO4, PO7, PO8, O1, O2 (Adam et al., 2018; Fukuda, Mance, & Vogel, 2015).

Change Detection Task Performance

The accuracy of all the participants for each set size was first calculated. The calculation of working memory capacity (K) for each set size in the change detection task followed the formula K = Set size × (Hit rate − False Alarm rate) / (1 − False Alarm rate) (Rouder, Morey, Morey, & Cowan, 2011), where hit rate represents proportion of correct responses on change trials and false alarm rate represents proportion of incorrect responses on no-change trials.

Experimental Design and Data Analysis

This experiment used a within-subject design with the two factors of set size (1, 3, vs. 6) and stimulus type (colored rectangles vs. letters). First, a two-way repeated-measures ANOVA was applied to accuracy and estimated capacity (K) across set sizes and stimulus types. Separate statistical analyses were then used to examine the CDA and alpha activity. First, the CDA amplitude and the lateralized alpha power following the presentation of each item were entered into separate repeated-measures ANOVAs for each set size with the within-subject factors of Stimulus Type (colored rectangles vs. letters) and Serial Position (e.g., first item, second item, vs. third item at set size 3; first item, second item, third item, fourth item, fifth item, vs. sixth item at set size 6). Next, we performed separate preplanned pairwise comparisons of CDA amplitude and lateralized alpha power across each neighboring serial position. All these statistical analyses were performed in SPSS 19.0 (IBM, Inc.).

RESULTS

Behavioral Results

As shown in Figure 2A, participants' memory accuracy for both colored rectangles and letters was at ceiling for set sizes 1 and 3, but dropped for set size 6. The two-way repeated-measures ANOVA on accuracy showed a significant Set Size effect, $F(2, 36) = 272.976$, $p < .001$, $\eta_p^2 = .938$. However, there was no effect of Stimulus Type, $F(1, 18) = 1.787$, $p = .198$, $\eta_p^2 = .090$, nor any interaction of Set Size × Stimulus Type, $F(2, 36) = 1.479$, $p = .241$, $\eta_p^2 = .076$. Follow-up tests using within-subject contrasts showed that working memory accuracy decreased from set size 1 (mean = 96.5% correct, SD = 0.6%) to set size 3 (mean = 90.7%, SD = 1.2%), $F(1, 18) = 44.761$, $p < .001$, $\eta_p^2 = .713$, and kept decreasing from set size 3 to set size 6 (mean = 71.3%, SD = 1.7%), $F(1, 18) = 399.985$, $p < .001$, $\eta_p^2 = .957$, for both colored rectangles and letters stimuli.

We also calculated K, an estimate of the number of items remembered, as shown in Figure 2B, and participants' memory for both colored rectangles and letters was near perfect at set sizes 1 and 3, but for set size 6, they could remember only about three of these objects. Thus, both measures of behavioral performance indicate

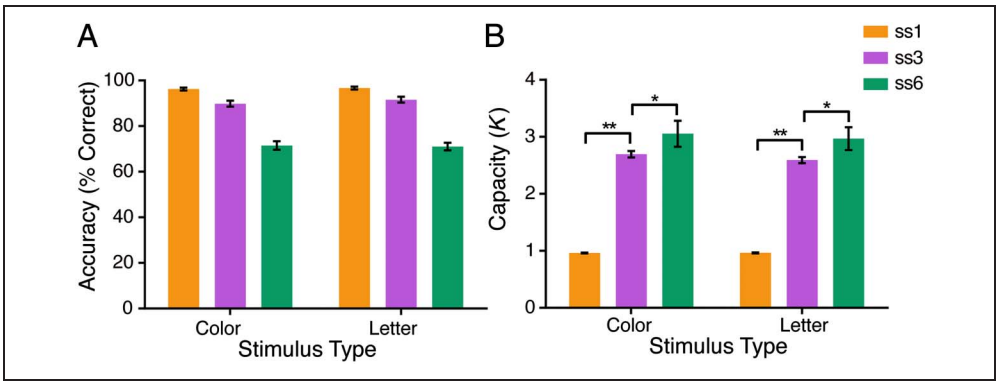

Figure 2. Behavioral performance across stimulus types and set sizes. (A) Mean accuracy and (B) capacity estimates for colored rectangles and letters across set sizes (orange, purple, and green bars represent set sizes 1, 3, and 6, respectively). Error bars indicate *SEM*. Asterisks indicate the significant differences between set sizes. *$p < .05$, **$p < .001$.

that we should see a metric of visual working memory storage increase until it hits capacity at about three objects' worth of information.

The two-way repeated-measures ANOVA on estimated capacity (K) showed a significant Set Size effect, $F(2, 36) = 104.513$, $p < .001$, $\eta_p^2 = .853$. However, there was no effect of Stimulus Type, $F(1, 18) = 0.012$, $p = .916$, $\eta_p^2 = .001$, nor any interaction of Set Size × Stimulus Type, $F(2, 36) = 0.984$, $p = .384$, $\eta_p^2 = .052$. Follow-up tests using within-subject contrasts showed that working memory capacity increased from set size 1 (mean = 0.963, $SD = 0.006$) to set size 3 (mean = 2.644, $SD = 0.050$), $F(1, 18) = 1280.379$, $p < .001$, $\eta_p^2 = .986$, and kept increasing from set size 3 to set size 6 (mean = 3.011, $SD = 0.200$), $F(1, 18) = 5.003$, $p = .038$, $\eta_p^2 = .217$, for both colored rectangles and letters stimuli.

CDA Results

Figure 3 illustrates the pattern of CDA activity that we observed. The CDA was found to increase in amplitude with each item, regardless of stimulus type, until visual working memory capacity was filled with about three items worth of information. This is seen most clearly in Figures 3B and 3C, where the contralateral negativity of the CDA is isolated with a difference wave, reaching asymptote at set size 3.

These observations about the behavior of the CDA were verified statistically in two ways. First, we calculated CDA amplitude following the presentation of each item (measured in the window of 300–700 msec poststimulus onset for the last stimulus, but 300–460 msec poststimulus onset for stimuli in other serial positions) by subtracting the ipsilateral voltage from the contralateral voltage and entered these into separate ANOVAs for each set size with the within-subject factors of Stimulus Types (colored rectangles vs. letters) and Serial Position (e.g., first item, second item, vs. third item at set size 3). For set size 3, the two-way repeated-measures ANOVA on CDA amplitude showed a significant Serial Position effect, $F(2, 36) = 32.288$, $p < .001$, $\eta_p^2 = .642$. However, there was no effect of Stimulus Type, $F(1, 18) = 0.754$, $p = .397$, $\eta_p^2 = .040$, or

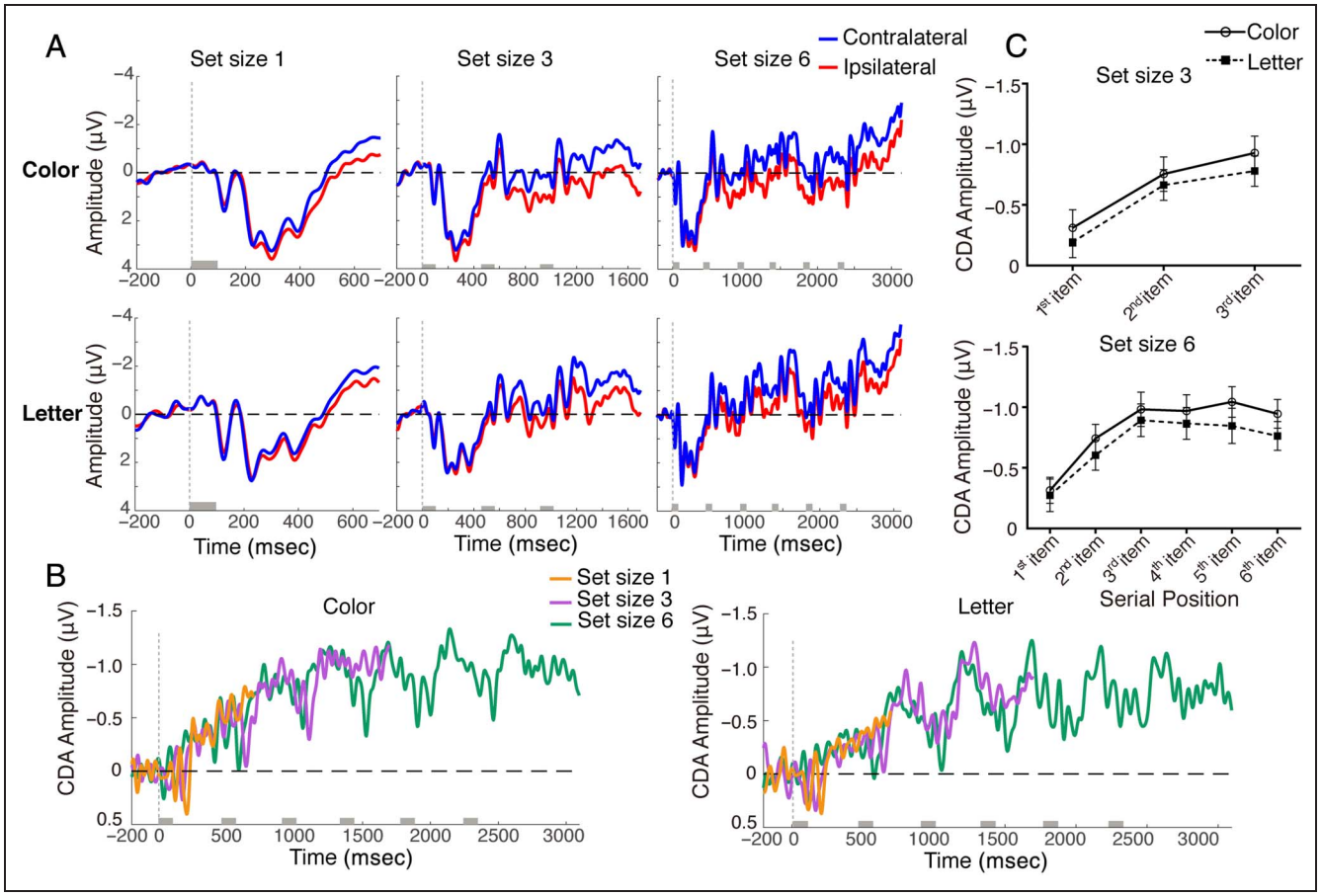

Figure 3. The CDA amplitude across stimulus types and set sizes. (A) ERP results. Contralateral (blue lines) and ipsilateral (red lines) waveforms from left to right for set sizes 1 to 6 and from upper to lower for colored rectangles and letters, averaged over electrode pairs: P3/4, P7/8, PO3/4, PO7/8, O1/2. The gray bars on the time axis represent the onset and duration of each memory array. (B) CDA waveforms (contralateral–ipsilateral) averaged over electrode pairs: P3/4, P7/8, PO3/4, PO7/8, O1/2, separated by set sizes (orange lines, purple lines, and green lines represent set sizes 1, 3, and 6, respectively) and stimulus type (left for colored rectangles and right for letters). The gray bars on the time axis represent the onset and duration of each memory array. (C) The mean CDA amplitude after each memory item in set size 3 (upper) and 6 (lower) conditions. Empty circles with solid lines and filled squares with dashed lines represent colored rectangles and letters, respectively. Error bars indicate *SEM*.

an interaction of Serial Position × Stimulus Type, $F(2, 36) = 0.486$, $p = .619$, $\eta_p^2 = .026$. Similarly, the two-way repeated-measures ANOVA on CDA amplitude at set size 6 showed a significant Serial Position effect, $F(5, 90) = 16.738$, $p < .001$, $\eta_p^2 = .482$. But there was neither an effect of Stimulus Type, $F(1, 18) = 3.263$, $p = .088$, $\eta_p^2 = .153$, nor any interaction of Serial Position × Stimulus Type, $F(5, 90) = 0.666$, $p = .650$, $\eta_p^2 = .036$. The asymptotic behavior of the CDA is evidenced by a significant effect of Serial Position at the set sizes that approach and exceed capacity (i.e., set sizes 3 and 6).

Next, we performed preplanned pairwise comparisons of CDA amplitude across each neighboring serial position. In these analyses, the point at which the CDA stops increasing will indicate when the asymptote was reached. Follow-up pairwise comparisons of CDA amplitude on set size 3 trials showed that the CDA amplitude increased from the first item to the second item, $F(1, 18) = 27.059$, $p < .001$, $\eta_p^2 = .601$. Consistent with participants' K scores, it kept increasing from the second item to the third item, $F(1, 18) = 6.718$, $p = .018$, $\eta_p^2 = .272$. For set size 6, pairwise comparisons of CDA amplitude showed that the CDA amplitude increased from the first item to the second item, $F(1, 18) = 26.534$, $p < .001$, $\eta_p^2 = .596$, kept increasing from the second item to the third item, $F(1, 18) = 33.422$, $p < .001$, $\eta_p^2 = .650$, but did not significantly change between the third and the fourth item, $F(1, 18) = 0.117$, $p = .736$, $\eta_p^2 = .006$, between the fourth item and the fifth item, $F(1, 18) = 0.376$, $p = .548$, $\eta_p^2 = .020$, and between the fifth item and the sixth item, $F(1, 18) = 1.411$, $p = .250$, $\eta_p^2 = .073$).

To provide stronger inferential power regarding the null results after the third item in the six-item sequence, we also computed Bayes factors (Rouder, Speckman, Sun, Morey, & Iverson, 2009). Across all of the paired-samples t tests of the CDA amplitude after the third item (the comparison between the third and the fourth item, the fourth and the fifth item, and the fifth and the sixth item for color stimuli and letter stimuli, respectively), the null hypothesis was 3.2 times (Bayes factors range from 1.8 to 4.1, mean = 3.2, $SD = 1.02$) more likely than the hypothesis that a difference existed between these items, demonstrating that we did not find a reliable change in CDA amplitude after the third item.

Neuroimaging studies have shown evidence for hemispheric specialization when verbal versus spatial information is maintained in working memory, with left hemisphere dominant for verbal storage and right hemisphere dominant for visuospatial storage (Walter et al., 2003; Smith, Jonides, & Koeppe, 1996). We analyzed the CDA amplitude in the left hemisphere (to-be-remembered items were presented on the right side of the screen) and the CDA amplitude in the right hemisphere (to-be-remembered items were presented on the left side of the screen) to examine whether there was a hemispheric lateralization of the CDA for the different stimuli. We entered the CDA amplitude elicited by set size 1 into a two-way repeated-measures ANOVA of within-subject factors of Hemisphere (left vs. right) × Stimulus Type (colored rectangles vs. letters). Then, we entered the CDA amplitudes elicited by set sizes 3 and 6 into separate three-way repeated-measures ANOVAs with the within-subject factors of Hemisphere (left vs. right) × Stimulus Type (colored rectangles vs. letters) × Serial Position (first item vs. second item vs. third item for set size 3, first item vs. second item vs. third item vs. fourth item vs. fifth item vs. sixth item for set size 6). The analyses revealed no main effect of Hemisphere with any of the set sizes: $F(1, 18) = 1.086$, $p = .311$, $\eta_p^2 = .057$, for set size 1; $F(1, 18) = 0.091$, $p = .767$, $\eta_p^2 = .005$, for set size 3; and $F(1, 18) = 0.076$, $p = .786$, $\eta_p^2 = .004$, for set size 6. Moreover, there was no interaction of Hemisphere × Stimulus Type with any of the set sizes, $F(1, 18) = 3.137$, $p = .093$, $\eta_p^2 = .148$, for set size 1; $F(1, 18) = 0.124$, $p = .728$, $\eta_p^2 = .007$, for set size 3; and $F(1, 18) = 0.334$, $p = .571$, $\eta_p^2 = .018$, for set size 6, or any interaction of Hemisphere × Stimulus Type × Serial Position, $F(2, 36) = 0.119$, $p = .889$, $\eta_p^2 = .007$, for set size 3, and $F(1, 18) = 2.053$, $p = .079$, $\eta_p^2 = .102$, for set size 6. Our results therefore did not provide evidence for hemispheric lateralization of the CDA amplitude with respect to the two types of stimuli we used in our task.

Alpha Results

Figure 4A illustrates the pattern of lateralized alpha activity that we observed. The lateralized alpha activity remained essentially constant with each item, regardless of stimulus type.

These observations about the behavior of the lateralized alpha power were verified by applying statistics that parallel the CDA analyses. We calculated lateralized alpha power following the presentation of each item (the same time window for CDA amplitude analyses) by subtracting the ipsilateral power from the contralateral power and entered these into separate ANOVAs for each set size with the within-subject factors of Stimulus Types (colored rectangles vs. letters) and Serial Position (e.g., first item, second item, vs. third item at set size 3). For set size 3, the two-way repeated-measures ANOVA on the lateralized alpha power showed that there was no effect of Serial Position, $F(2, 36) = 1.797$, $p = .180$, $\eta_p^2 = .091$; no effect of Stimulus Type, $F(1, 18) = 0.082$, $p = .778$, $\eta_p^2 = .005$; nor any interaction of Serial Position × Stimulus Type, $F(2, 36) = 0.114$, $p = .892$, $\eta_p^2 = .006$. Similarly, the two-way repeated-measures ANOVA on lateralized alpha power in set size 6 condition showed that there was no effect of Serial Position, $F(5, 90) = 1.027$, $p = .407$, $\eta_p^2 = .054$, no effect of Stimulus Type, $F(1, 18) = 0.710$, $p = .411$, $\eta_p^2 = .038$, nor any interaction of Serial Position × Stimulus Type, $F(5, 90) = 1.109$, $p = .361$, $\eta_p^2 = .058$. In addition, none of the preplanned pairwise comparisons of alpha power across serial position was significant (ps > .162), except a significant difference between the fifth item and the sixth item in set size 6 condition, $F(1, 18) = 4.775$, $p = .042$, $\eta_p^2 = .210$. These null effects of Serial Position on

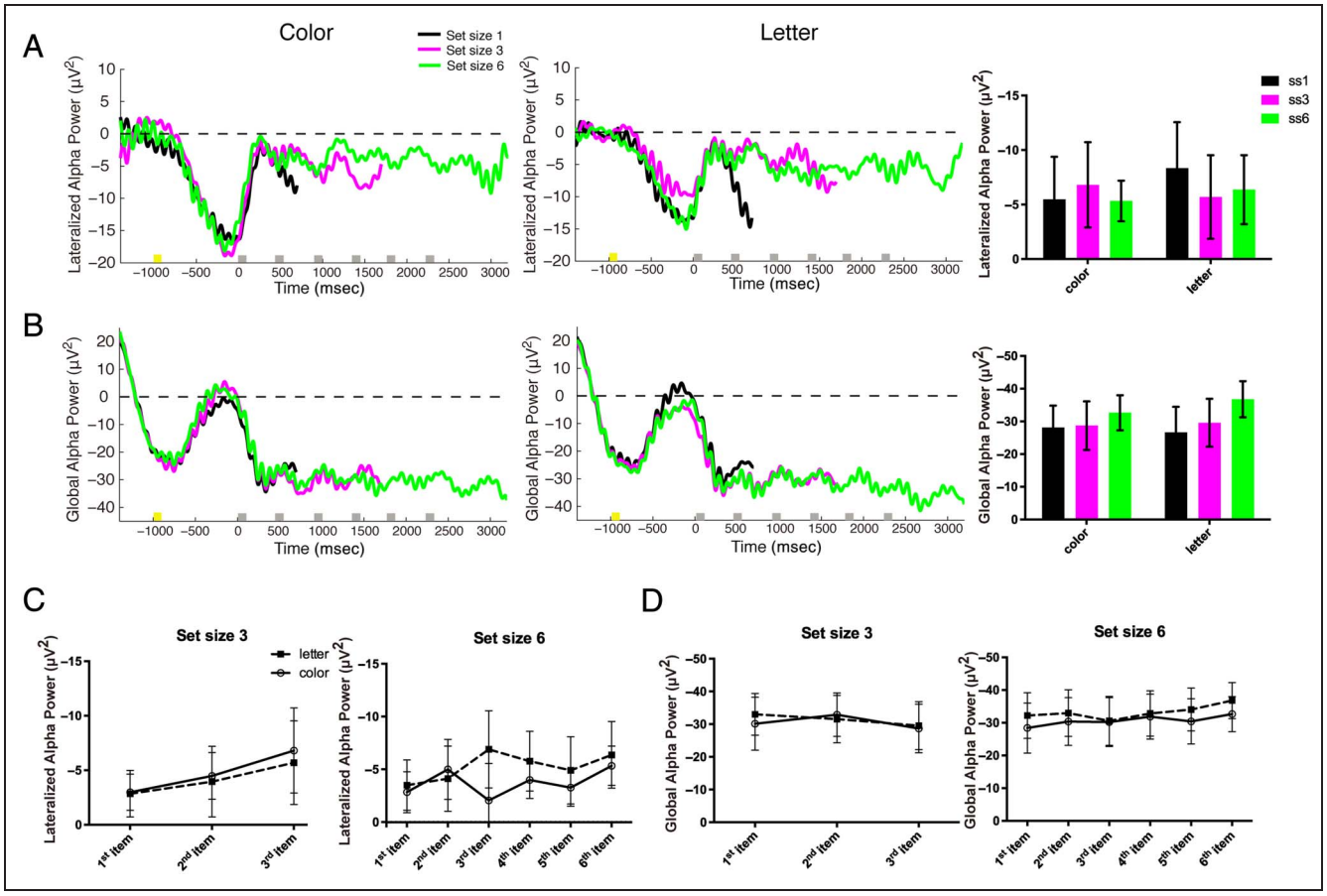

Figure 4. The lateralized and global alpha power across stimulus types and set sizes. (A) Lateralized alpha power (contralateral–ipsilateral) averaged over electrode pairs: P3/4, P7/8, PO3/4, PO7/8, O1/2, separated by set sizes (black lines, magenta lines, and green lines represent set sizes 1, 3, and 6, respectively) and stimulus type (left for colored rectangles and right for letters). The gray bars on the time axis represent the onset and duration of each memory array; the yellow bars show the onset and duration of the cue array. The bar graph represents the mean lateralized alpha power time-locked to the last sample onset (black bars, magenta bars, and green bars represent set sizes 1, 3, and 6, respectively). (B) Global alpha power averaged over electrode pairs: P3/4, P7/8, PO3/4, PO7/8, O1/2, separated by set sizes (black lines, magenta lines, and green lines represent set sizes 1, 3, and 6, respectively) and stimulus type (left for colored rectangles and right for letters). The gray bars on the time axis represent the onset and duration of each memory array. The yellow bars show the onset and duration of the cue array. The bar graph represents the mean global alpha power time-locked to the last sample onset (black bars, magenta bars, and green bars represent set sizes 1, 3, and 6, respectively). (C) Mean lateralized alpha power for each memory array in set size 3 (left) and 6 (right) conditions. (D) Mean global alpha power for each memory array in set size 3 (left) and 6 (right) conditions. Empty circles with solid lines and filled squares with dashed lines represent colored rectangles and letters, respectively. Error bars indicate *SEM*.

lateralized alpha power suggest that the lateralized alpha power remained constant as more objects were stored.

A recent study suggests that the alpha power suppression may last much longer than the CDA amplitude during long retention intervals (Fukuda et al., 2015). To address the possibility that the null effects of serial position on alpha was due to the limited retention intervals during our sequential presentation task, we compared lateralized alpha power time-locked to the last sample across set sizes, because the time between the last item and the test array afforded the longest measurement window in our design. A two-way repeated-measures ANOVA with within-subject factors of Set Size (1, 3, and 6) and Stimulus Type (colored rectangles, letters) was applied to the lateralized alpha power after the last sample array onset (300–700 msec). The analysis showed that there was no effect of Set Size, $F(2, 36) = 0.204$, $p = .816$, $\eta_p^2 = .011$, no effect of Stimulus Type, $F(1, 18) = 0.476$, $p = .499$, $\eta_p^2 = .026$, and no interaction of Set Size × Stimulus Type, $F(2, 36) = 0.900$, $p = .416$, $\eta_p^2 = .048$. In addition, none of the preplanned pairwise comparisons of alpha power across set size was significant ($ps > .509$).

A number of recent studies have shown that the global alpha power across all posterior electrodes tracks the number of items stored in visual working memory (Adam et al., 2018; Fukuda et al., 2015, 2016). So we next examined whether global alpha power increased sequentially across the sequentially presented items. As shown in Figure 4B, our measurements of global alpha power suggest that it remained essentially constant as more objects were stored, regardless of stimulus type.

We calculated global alpha power following the presentation of each item by averaging across all the posterior electrodes and entered these into separate ANOVAs for

each set size with the within-subject factors of Stimulus Type (colored rectangles vs. letters) and Serial Position (e.g., first item, second item, vs. third item at set size 3). For set size 3, the two-way repeated-measures ANOVA on global alpha power showed that there was no effect of Serial Position, $F(2, 36) = 1.022$, $p = .370$, $\eta_p^2 = .054$, no effect of Stimulus Type, $F(1, 18) = 0.441$, $p = .515$, $\eta_p^2 = .024$, and no interaction of Serial Position × Stimulus Type, $F(2, 36) = 0.810$, $p = .453$, $\eta_p^2 = .043$. Similarly, the two-way repeated-measures ANOVA on global alpha power measured across stimuli with a set size of 6 showed that there was no effect of Serial Position, $F(5, 90) = 0.665$, $p = .651$, $\eta_p^2 = .036$; no effect of Stimulus Type, $F(1, 18) = 2.584$, $p = .125$, $\eta_p^2 = .126$; and no interaction of Serial Position × Stimulus Type, $F(5, 90) = 1.019$, $p = .411$, $\eta_p^2 = .054$. In addition, none of the preplanned pairwise comparisons of alpha power across serial position were significant (ps > .057). To parallel analyses of lateralized alpha power and to exclude the possibility that the null effects of serial position are due to the limited delay time of the earlier serial positions, we entered the measures of global alpha power after the last sample array onset (300–700 msec) into a two-way repeated-measures ANOVA with within-subject factors of Set Size (1, 3, vs. 6) and Stimulus Type (colored rectangles vs. letters). The analysis showed that there was no effect of Set Size, $F(2, 36) = 2.553$, $p = .092$, $\eta_p^2 = .124$; no effect of Stimulus Type, $F(1, 18) = 0.507$, $p = .485$, $\eta_p^2 = .027$; and no significant interaction of Set Size × Stimulus Type, $F(2, 36) = 2.097$, $p = .138$, $\eta_p^2 = .104$. Finally, none of the preplanned pairwise comparisons of alpha power across set size were significant (ps > .093).

It is possible that the alpha-band signal is less reliable than the CDA component measured at the same time, across the same trials. This might explain why the CDA shows clear effects of the sequentially presented objects, whereas the alpha-band activity does not. To address this, we also computed Bayes factors to determine how much more likely the null hypothesis was than the possibility that alpha-band activity actually did show an effect (Rouder, Morey, Verhagen, Swagman, & Wagenmakers, 2017). We found that, for the effect of serial position on lateralized alpha power, the null hypothesis was 2.5 times more likely at set size 3 and 2436.8 times more likely at set size 6 than the hypothesis that a difference existed. Similarly, across all of the pairwise comparisons of alpha activity, the null hypothesis was 3.9 times (Bayes factors range from 1.2 to 4.0, mean = 2.5, $SD = 0.97$) more likely than the hypothesis that a difference existed. For the effect of serial position on global alpha power, the null hypothesis was 3.6 times and 17.5 times more likely than the hypothesis that a difference existed at set size 3 and set size 6, respectively. Similarly, across all of the pairwise comparisons of alpha activity, the null hypothesis was 2.6 times (Bayes factors range from 0.3 to 4.0, mean = 2.6, $SD = 1.14$) more likely than the hypothesis that a difference existed. These analyses demonstrate that our comparisons of alpha-band activity across the serial positions were not simply limited by power, but instead there was a convincing null result on alpha power, across the to-be-remembered items.

DISCUSSION

In the current study, we measured two neural indices that have been identified by presenting participants with arrays containing multiple to-be-remembered objects. The CDA and lateralized alpha oscillations of the human brain have been proposed to measure the storage of information in visual working memory. Our results showed that the amplitude of CDA increased following the presentation of each to-be-remembered object, reaching asymptote at about three to four objects. In contrast, the lateralized alpha power that was measured concurrently remained constant with each additional object. These results show that the CDA tracks the storage of objects in visual working memory, whereas lateralized alpha suppression more likely indexes the focusing of attention on the to-be-remembered objects.

Our experiment suggests that the CDA alone grows with the presentation of single items and reaches a plateau after capacity has been exceeded, as would be expected of a neural metric of visual working memory capacity. It is difficult to explain the CDA activity we observed with an attentional account, given that the number of stimuli that needed to be attended was constant at each point in time. Indeed, consolidation rate estimates suggest that the delay between stimuli in our experiment provided ample time for encoding and consolidation processes to finish between stimuli (Vogel, Woodman, & Luck, 2006; Woodman & Vogel, 2005). For this reason, we believe that our results rule out an explanation of the CDA in terms of the demand on spatial attention during encoding. Although it may be tempting to suggest that the CDA instead reflects sustained attention to multiple locations during the retention interval, this is inconsistent with the results of Ikkai, McCollough, and Vogel (2010), who found no difference in the CDA when two pairs of objects appeared at the same or different locations. However, because our experiment involved only a single relevant hemifield on each trial, we cannot rule out the possibility that the CDA reflects an internal, hemifield-specific spatial focus of attention that maintains object representations (Berggren & Eimer, 2016; see Feldmann-Wüstefeld, Vogel, & Awh, 2018, for an additional account of hemifield-switching results).

Time and set size are inherently confounded in paradigms using sequential presentation and varying the size of the memory set. A reader may worry that the set size effects are simply due to differential passage of time between the start of the trial and the onset of the test array. Fortunately, we can reject the explanation that the present findings are simply due to a time confound for the

following reasons. First, this inherent confound of time and sequence length is an issue addressed in a previous work showing minimal differences caused by the different retention intervals relative to the huge set size effects using color change detection tasks identical to those used here (Woodman, Vogel, & Luck, 2012). Second, to explain the data from set size 3 and 6 sequences, a time-based explanation of the results needs to propose that the CDA inherently increases for over a second, then reaches asymptote at a high level, and maintains that level for another couple of seconds. However, previous CDA experiments do not show a 1500-msec phase of increase, followed by a 1500-msec plateau, as Figure 3 shows, is necessary to explain the CDA results (Fukuda et al., 2016; Luria et al., 2016; Carlisle, Arita, Pardo, & Woodman, 2011; Woodman & Vogel, 2008; Vogel et al., 2005; Vogel & Machizawa, 2004).

Previous work has shown that lateralized alpha power suppression is greater for later set sizes in memory tasks (Sauseng et al., 2009; but see Fukuda et al., 2016). Because of this, some researchers have proposed that the CDA and lateralized alpha power might reflect the same neural processes of visual working memory storage (van Dijk, van der Werf, Mazaheri, Medendorp, & Jensen, 2010). However, unlike the strong accumulation effect we observed on the CDA as more stimuli were encoded, there was no accumulation effect on lateralized alpha power in our sequential working memory task. Contrary to the suggestion that the CDA is produced by asymmetric lateralized alpha power (van Dijk et al., 2010), our results suggest that the CDA and lateralized alpha power reflect dissociable cognitive functions. The CDA reflects visual working memory storage, whereas lateralized alpha power represents the focusing of spatial attention on an item or on an array of items. Previous findings of an increase in alpha lateralization with higher set sizes may reflect the need to attend to multiple locations when memory sets are presented simultaneously or retrieved from long-term memory as a group. Overall, our findings are consistent with previous studies that suggest that the CDA and lateralized alpha power measure dissociable functions (Hakim et al., 2019; Fukuda et al., 2015, 2016).

An expert in the study of working memory may be interested in how alpha-band activity and the CDA would have behaved if we would have used a continuous report task that allows for modeling of the precision of the participants' memory representations. For example, Gorgoraptis, Catalao, Bays, and Husain (2011) recently used the sequential presentation of colored bars and asked their participants to recall the orientation of one of the sequentially presented colored bars as precisely as possible. Their results showed a clear recency effect: The fidelity of the last item was significantly more precise than preceding items, regardless of memory load. However, no differences in precision were observed for earlier positions in a sequence (from three to five items). Their results suggest that the items presented in a sequence might be accurately encoded, except that the last item benefits from a recency effect. The present data suggest that this recency effect might be due to the final memory representation benefitting from being both the focus of attention (i.e., indexed by alpha-band activity) and held in working memory (i.e., indexed by the CDA). This is an interesting direction for future research to address the long-standing question of the nature of serial position effects.

In conclusion, we measured two neural indices, the CDA and lateralized alpha oscillations, to determine whether these neural indices track the same cognitive mechanism or different mechanisms in the human brain. Our results showed that the CDA amplitude rose with the number of items stored in visual working memory, and it reached a plateau after reaching the visual working memory capacity limit for both colored rectangles and letters. Meanwhile, lateralized alpha power remained constant with more items stored in visual working memory regardless of stimulus type. Together, these results indicate that the CDA tracks the number of representations in visual working memory during dynamic encoding and storage, whereas lateralized alpha power reflects the locus of spatial attention instead of visual working memory storage. Thus, the ERP and the oscillatory activity measured at the same time do not appear to be different manifestations of the same cognitive mechanism at work in the human brain, but instead, these different signals appear to index different cognitive operations.

Acknowledgments

The present work was supported by grants from the National Institutes of Health (R01-EY019882, R01-EY025275, R01-MH110378, P30-EY08126, and T32-EY007135) to G. F. W. and the China Scholarship Council scholarship (201706140083) to S. W. We also thank David W. Sutterer for his useful discussions.

Reprint requests should be sent to Geoffrey F. Woodman, Department of Psychology, Vanderbilt University, Nashville, TN, 37240, or via e-mail: geoffrey.f.woodman@vanderbilt.edu.

REFERENCES

Adam, K. C. S., Robison, M. K., & Vogel, E. K. (2018). Contralateral delay activity tracks fluctuations in working memory performance. *Journal of Cognitive Neuroscience*, *30*, 1229–1240.

Baddeley, A. D., & Hitch, G. (1974). Working memory. In G. H. Bower (Ed.), *The psychology of learning and motivation: Advances in research and theory* (pp. 47–89). New York: Academic Press.

Berggren, N., & Eimer, M. (2016). Does contralateral delay activity reflect working memory storage or the current focus of spatial attention within visual working memory? *Journal of Cognitive Neuroscience*, *28*, 2003–2020.

Brainard, D. H. (1997). The psychophysics toolbox. *Spatial Vision*, *10*, 433–436.

Broadbent, D. E., & Broadbent, M. H. (1981). Recency effects in visual memory. *Quarterly Journal of Experimental Psychology, Section A: Human Experimental Psycholgy*, *33*, 1–15.

Brown, J. (1958). Some tests of the decay theory of immediate memory. *Quarterly Journal of Experimental Psychology*, *10*, 12–21.
Carlisle, N. B., Arita, J. T., Pardo, D., & Woodman, G. F. (2011). Attentional templates in visual working memory. *Journal of Neuroscience*, *31*, 9315–9322.
Conrad, R. (1964). Acoustic confusions in immediate memory. *British Journal of Psychology*, *55*, 75–84.
Cowan, N. (2001). The magical number 4 in short-term memory: A reconsideration of mental storage capacity. *Behavioral and Brain Sciences*, *24*, 87–114.
Delorme, A., & Makeig, S. (2004). EEGLAB: An open source toolbox for analysis of single-trial EEG dynamics including independent component analysis. *Journal of Neuroscience Methods*, *134*, 9–21.
Feldmann-Wüstefeld, T., Vogel, E. K., & Awh, E. (2018). Contralateral delay activity indexes working memory storage, not the current focus of spatial attention. *Journal of Cognitive Neuroscience*, *30*, 1185–1196.
Fukuda, K., Kang, M.-S., & Woodman, G. F. (2016). Distinct neural mechanisms for spatially lateralized and spatially global visual working memory representations. *Journal of Neurophysiology*, *116*, 1715–1727.
Fukuda, K., Mance, I., & Vogel, E. K. (2015). α power modulation and event-related slow wave provide dissociable correlates of visual working memory. *Journal of Neuroscience*, *35*, 14009–14016.
Gorgoraptis, N., Catalao, R. F. G., Bays, P. M., & Husain, M. (2011). Dynamic updating of working memory resources for visual objects. *Journal of Neuroscience*, *31*, 8502–8511.
Hakim, N., Adam, K. C. S., Gunseli, E., Awh, E., & Vogel, E. K. (2019). Dissecting the neural focus of attention reveals distinct processes for spatial attention and object-based storage in visual working memory. *Psychological Science*, *30*, 526–540.
Ikkai, A., McCollough, A. W., & Vogel, E. K. (2010). Contralateral delay activity provides a neural measure of the number of representations in visual working memory. *Journal of Neurophysiology*, *103*, 1963–1968.
Kelly, S. P., Lalor, E. C., Reilly, R. B., & Foxe, J. J. (2006). Increases in alpha oscillatory power reflect an active retinotopic mechanism for distracter suppression during sustained visuospatial attention. *Journal of Neurophysiology*, *95*, 3844–3851.
Luria, R., Balaban, H., Awh, E., & Vogel, E. K. (2016). The contralateral delay activity as a neural measure of visual working memory. *Neuroscience & Biobehavioral Reviews*, *62*, 100–108.
McCollough, A. W., Machizawa, M. G., & Vogel, E. K. (2007). Electrophysiological measures of maintaining representations in visual working memory. *Cortex*, *43*, 77–94.
Pelli, D. G. (1997). The VideoToolbox software for visual psychophysics: Transforming numbers into movies. *Spatial Vision*, *10*, 437–442.
Rouder, J. N., Morey, R. D., Morey, C. C., & Cowan, N. (2011). How to measure working memory capacity in the change detection paradigm. *Psychonomic Bulletin & Review*, *18*, 324–330.
Rouder, J. N., Morey, R. D., Verhagen, J., Swagman, A. R., & Wagenmakers, E.-J. (2017). Bayesian analysis of factorial designs. *Psychological Methods*, *22*, 304–321.
Rouder, J. N., Speckman, P. L., Sun, D., Morey, R. D., & Iverson, G. (2009). Bayesian *t* tests for accepting and rejecting the null hypothesis. *Psychonomic Bulletin & Review*, *16*, 225–237.
Sander, M. C., Werkle-Bergner, M., & Lindenberger, U. (2012). Amplitude modulations and inter-trial phase stability of alpha-oscillations differentially reflect working memory constraints across the lifespan. *Neuroimage*, *59*, 646–654.
Sauseng, P., Klimesch, W., Heise, K. F., Gruber, W. R., Holz, E., Karim, A. A., et al. (2009). Brain oscillatory substrates of visual short-term memory capacity. *Current Biology*, *19*, 1846–1852.
Sauseng, P., Klimesch, W., Stadler, W., Schabus, M., Doppelmayr, M., Hanslmayr, S., et al. (2005). A shift of visual spatial attention is selectively associated with human EEG alpha activity. *European Journal of Neuroscience*, *22*, 2917–2926.
Smith, E. E., Jonides, J., & Koeppe, R. A. (1996). Dissociating verbal and spatial working memory using PET. *Cerebral Cortex*, *6*, 11–20.
Sternberg, S. (1969). Memory-scanning: Mental processes revealed by reaction-time experiments. *American Scientist*, *57*, 421–457.
Thut, G., Nietzel, A., Brandt, S. A., & Pascual-Leone, A. (2006). α-band electroencephalographic activity over occipital cortex indexes visuospatial attention bias and predicts visual target detection. *Journal of Neuroscience*, *26*, 9494–9502.
van Dijk, H., van der Werf, J., Mazaheri, A., Medendorp, W. P., & Jensen, O. (2010). Modulations in oscillatory activity with amplitude asymmetry can produce cognitively relevant event-related responses. *Proceedings of the National Academy of Sciences, U.S.A.*, *107*, 900–905.
Vogel, E. K., & Machizawa, M. G. (2004). Neural activity predicts individual differences in visual working memory capacity. *Nature*, *428*, 748–751.
Vogel, E. K., McCollough, A. W., & Machizawa, M. G. (2005). Neural measures reveal individual differences in controlling access to working memory. *Nature*, *438*, 500–503.
Vogel, E. K., Woodman, G. F., & Luck, S. J. (2006). The time course of consolidation in visual working memory. *Journal of Experimental Psychology: Human Perception and Performance*, *32*, 1436–1451.
Walter, H., Bretschneider, V., Grön, G., Zurowski, B., Wunderlich, A. P., Tomczak, R., et al. (2003). Evidence for quantitative domain dominance for verbal and spatial working memory in frontal and parietal cortex. *Cortex*, *39*, 897–911.
Woodman, G. F., & Luck, S. J. (2003). Serial deployment of attention during visual search. *Journal of Experimental Psychology: Human Perception and Performance*, *29*, 121–138.
Woodman, G. F., & Vogel, E. K. (2005). Fractionating working memory: Consolidation and maintenance are independent processes. *Psychological Science*, *16*, 106–113.
Woodman, G. F., & Vogel, E. K. (2008). Selective storage and maintenance of an object's features in visual working memory. *Psychonomic Bulletin & Review*, *15*, 223–229.
Woodman, G. F., Vogel, E. K., & Luck, S. J. (2012). Flexibility in visual working memory: Accurate change detection in the face of irrelevant variations in position. *Visual Cognition*, *20*, 1–28.
Worden, M. S., Foxe, J. J., Wang, N., & Simpson, G. V. (2000). Anticipatory biasing of visuospatial attention indexed by retinotopically specific α-band electroencephalography increases over occipital cortex. *Journal of Neuroscience*, *20*, RC63.